Connection of envelope functions at semiconductor heterointerfaces. I. Interface matrix calculated in simplest models

T. Ando, S. Wakahara, and H. Akera
Institute for Solid State Physics, University of Tokyo, 7-22-1 Roppongi, Minato-ku, Tokyo 106, Japan
(Received 21 February 1989; revised manuscript received 21 June 1989)

The boundary conditions for the envelope functions at semiconductor heterointerfaces are calculated. They are obtained in a form of a 2×2 interface matrix, which gives two linear relations among the envelopes and their derivatives at interfaces. The two models considered are a linear-chain tight-binding model consisting of a cation s orbital and an anion p orbital and an empirical pseudopotential model containing a small number of basis plane waves. The results show that the so-called envelope-function approximation works surprisingly well in various heterostructures, including GaAs/$Al_xGa_{1-x}As$, HgTe/CdTe, and GaSb/InAs.

I. INTRODUCTION

The most commonly and widely used method for determining electronic states in bulk semiconductors is the effective-mass approximation. In the effective-mass approximation, the wave function appearing in the Schrödinger equation is not the total wave function but its envelope of the Bloch functions varying rapidly within each unit cell.[1] It has now become possible to synthesize semiconductor heterostructures such as heterojunctions, quantum wells, and superlattices having a good quality, owing to development of crystal-growth technologies. The conventional effective-mass approximation is not directly applicable to such heterostructures, because the potential varies strongly within the distance of the lattice constant in the vicinity of interfaces. Effects of such heterointerfaces can be incorporated only in the form of boundary conditions for envelope functions. The purpose of the present paper is to present such boundary conditions calculated in simple models.

Since the first proposal by Esaki and Tsu,[2] the semiconductor heterostructure has caught attention from the viewpoint of pure physics, materials science, and device applications. From the point of view of pure physics, the heterostructure provides various elemental problems including band-gap alignment[3] and matching of wave functions at heterointerfaces. In addition, the heterostructure has also produced a two-dimensional electron system having a supreme quality, where the famous fractional quantum Hall effect was observed for the first time.[4] In device application, the high-electron-mobility transistor,[5] quantum-well laser,[6] and various resonant tunneling devices[7–9] are being pursued.

There has been a rapid development in first-principles calculation of band structure of semiconductors.[10–14] However, its complexity prevents a wide application and the accuracy is limited to the order of at best 100 meV, which is still much larger than the accuracy of 1–10 meV required for various purposes. In the case of superlattices, various empirical models such as pseudopotentials[15–20] and tight-binding models[21–18] may also be used. It is almost impossible, however, to uniquely choose parameters characterizing the model so as to exactly reproduce corresponding bulk-band structure. Further, the results of such direct band-structure calculations are not so useful except in discussing optical properties such as direct absorption and luminescence.

The effective-mass approximation has advantages as compared to direct tight-binding or empirical pseudopotential calculations even in just determining electronic energy levels in heterostructures. It can easily be applied to a self-consistent calculation in the presence of band bending due to charge redistribution.[29,30] Further, it is ideal for the study of effects of slowly varying perturbations such as the electron-hole Coulomb potential in exciton problems, impurity potentials, electric and magnetic fields, etc.[31] In discussing transport properties such as galvanomagnetic effects and hot electrons and in performing device simulations, the use of the effective-mass description is almost imperative.

There have been extensive experimental and theoretical investigations on electronic properties of GaAs/$Al_xGa_{1-x}As$ heterostructures.[32] In these systems, the so-called envelope-function approximation (EFA) has turned out to work surprisingly well in determining conduction-band energy levels. In the EFA the envelope itself is continuous across the interfaces but its derivative is discontinuous in such a way that the flux conservation is satisfied.[33,34] This EFA has been extended to multiband cases.[35–38] The basic assumption of deriving the EFA is that band-edge Bloch functions are identical on both sides of the interface.[35] However, the band-edge (the conduction-band bottom, for example) wave functions of various semiconductors are not identical, although they have the same symmetry. It remains still unclear, therefore, why the EFA is valid in wide varieties of heterostructures achieved experimentally so far.

There have been several important contributions to the problem of boundary conditions on the envelope function.[39–46] Various schemes of characterizing boundary conditions have been proposed[41–43] and there have been attempts to characterize interfaces with transmission and reflection coefficients.[45,46] It has also been pointed out

that varieties of boundary conditions can exist which cannot be expressed only by the effective-mass parameters such as the effective mass and the band gap.[44] However, most of these works considered only unrealistic one-dimensional models or are insufficient in full description of boundary conditions (transmission-reflection coefficients, for example, depend directly on energy of incident electrons and band offsets and are not suitable in fully characterizing boundary conditions), and basic features have not been clarified yet. In the present paper, we employ two models, which in spite of their simplicity can reproduce main features of the band structure of III-V and II-VI compound semiconductors in the vicinity of the Γ point, and try to obtain some insight into the question of the validity of the EFA. The first model is a linear-chain tight-binding model consisting of a cation s orbital, an anion p, and a nearest-neighbor transfer integral. The second is an empirical pseudopotential model containing a small number of basis plane waves. Extension to interesting and important problems directly related to mixings between Γ and X conduction-band minima in $GaAs/Al_xGa_{1-x}As$, such as resonant tunneling through Γ-X-Γ valleys, is given in the following paper.

This paper is organized as follows. In Sec. II the interface matrix T_{BA} is introduced, which gives boundary conditions for envelopes, i.e., linear relations among envelopes and their derivatives at the interface. Various properties of the interface matrix are reviewed briefly. In Sec. III the interface matrix is calculated within a linear-chain tight-binding model for various types of connections of envelopes, i.e., between conduction bands, between valence bands, and between conduction and valence bands. Explicit results are obtained for the interface matrix of $GaAs/Al_xGa_{1-x}As$, HgTe/CdTe, and GaSb/InAs heterostructures. It is shown that the EFA works surprisingly well in these systems. In Sec. IV the interface matrix for the Γ conduction-band bottom is calculated in an empirical pseudopotential model. The results depend on the position of the interface or the matching plane, but deviation from the EFA is not important, again justifying the use of the EFA. Some of the results given in Secs. II and III have already been presented elsewhere,[47] but are included for the sake of completeness and convenience. A very preliminary account of the results in Sec. IV has also been given.[48]

II. INTERFACE MATRIX

Let us consider an interface of a semiconductor A occupying the left ($z<0$) half-space and B occupying the right ($z>0$) half-space. We consider the case that both semiconductor A and B possess a single band maximum or minimum which lies close in energy, and discuss energy levels close to the band extrema and corresponding wave functions. In bulk semiconductors, these states are described well by the powerful effective-mass approximation in which the envelope of the Bloch function satisfies a second-order differential equation. In the presence of heterointerfaces, the wave functions of A and B should match smoothly with each other at the interface ($z=0$). This does not necessarily mean that associated envelope functions are continuous across the interface. However, if the envelope in A is given, that of B is uniquely determined. This fact can be described by the following linear relation between envelopes and their derivatives at $z=0$:

$$\begin{bmatrix} \zeta_B(0) \\ \nabla\zeta_\beta(0) \end{bmatrix} = T_{BA} \begin{bmatrix} \zeta_A(0) \\ \nabla\zeta_A(0) \end{bmatrix} \tag{2.1}$$

with $\nabla = a(\partial/\partial z)$ and a the lattice constant, where $T_{BA}=(t_{ij})$ is a 2×2 matrix which will be called the interface matrix.

All the matrix elements of T_{BA} are not independent of each other because the boundary conditions should satisfy the conditions for flux conservation at the interface. In terms of the envelope function the flux is written as

$$j(z)=\frac{\hbar}{2im}\left[\zeta^*(z)\frac{\partial}{\partial z}\zeta(z)-\left[\frac{\partial}{\partial z}\zeta^*(z)\right]\zeta(z)\right] \tag{2.2}$$

with m the effective mass. Therefore, the flux conservation condition is written in terms of T_{BA} as

$$T_{BA}^{+}\begin{bmatrix} 0 & 1/m_B \\ -1/m_B & 0 \end{bmatrix} T_{BA} = \begin{bmatrix} 0 & 1/m_A \\ -1/m_A & 0 \end{bmatrix}, \tag{2.3}$$

where T_{BA}^{+} is the Hermitian conjugate of T_{BA}, and m_A and m_B are the effective mass of the semiconductor A and B, respectively. This relation leads to the conclusion that t_{ij} can be chosen as real except for a common phase factor and

$$\det T_{BA}=\frac{m_B}{m_A}\ . \tag{2.4}$$

Instead of T_{BA} we may define $\tilde{T}_{BA}=(\tilde{t}_{ij})$ by the relation

$$\begin{bmatrix} \zeta_B(0) \\ \nabla_B\zeta_B(0) \end{bmatrix} = \tilde{T}_{BA} \begin{bmatrix} \zeta_A(0) \\ \nabla_A\zeta_A(0) \end{bmatrix}, \tag{2.5}$$

where $\nabla_A=(m_0/m_A)\nabla$ and $\nabla_B=(m_0/m_B)\nabla$ with m_0 the free electron mass. The flux conservation now reads

$$\tilde{T}_{BA}^{+}\begin{bmatrix} 0 & 1 \\ -1 & 0 \end{bmatrix}\tilde{T}_{BA}=\begin{bmatrix} 0 & 1 \\ -1 & 0 \end{bmatrix} \quad \text{or} \quad \det\tilde{T}_{BA}=1\ . \tag{2.6}$$

The elements of T_{BA} and $\tilde{T}_{BA}$ are related to each other through

$$\begin{aligned} \tilde{t}&=t_{11}\ , \\ \tilde{t}_{12}&=\frac{m_A}{m_0}t_{12}\ , \\ \tilde{t}_{21}&=\frac{m_0}{m_B}t_{21}\ , \end{aligned} \tag{2.7}$$

and

$$\tilde{t}_{22}=\frac{m_A}{m_B}t_{22}\ .$$

In order to obtain the interface matrix, we have to perform interface calculations from first principles or based

on some models which can reasonably reproduce band structure of corresponding bulk materials. In either case, it is very hard to reproduce known effective masses exactly. It is more convenient, therefore, to calculate $\tilde{T}_{BA}$ instead of T_{BA} because the flux conservation condition for the former matrix does not contain effective masses explicitly. We can then use known effective masses, band offsets, and $\tilde{T}_{BA}$ in actual calculations of energy levels and obtain results satisfying the flux conservation.

The interface matrix can describe various kinds of boundary conditions. Among various elements t_{21} is most important, because it is related to the presence of interface states. To see this, we consider a uniform system in which a δ-function potential is present at $z=0$ as has been considered by Zhu and Kroemer,[41] i.e.,

$$\left[-\frac{\hbar^2}{2m}\frac{\partial^2}{\partial z^2}+V_0\delta(z)\right]\zeta(z)=E\zeta(z)\ . \tag{2.8}$$

It is straightforward to see that the δ-function potential can be incorporated into the interface matrix T_{BA} given by

$$T_{BA}=\begin{bmatrix}1 & 0\\ 2maV_0/\hbar^2 & 1\end{bmatrix}\ . \tag{2.9}$$

This shows that the positive t_{21} roughly corresponds to the presence of a repulsive δ-function potential and leads to the reduction of the envelope function at the interface. The negative t_{21}, on the other hand, corresponds to an attractive δ-function potential and leads to the increase of the envelope at the interface, often giving rise to a bound interface state.

On the other hand, t_{12} plays a minor role except in the case that other elements are extremely small or in the case $t_{12}\gg 1$. Suppose that we choose the interface position at $z=\delta z$ with $|\delta z|\lesssim a$ instead of $z=0$. Then, the same boundary conditions are expressed by the new interface matrix $T_{BA}(\delta z)$ as

$$\begin{bmatrix}\zeta_B(\delta z)\\ \nabla\zeta_B(\delta z)\end{bmatrix}=T_{BA}(\delta z)\begin{bmatrix}\zeta_A(\delta z)\\ \nabla\zeta_A(\delta z)\end{bmatrix}\ , \tag{2.10}$$

where

$$T_{BA}(\delta z)=\begin{bmatrix}t_{11}+t_{21}\delta & t_{12}-t_{11}\delta+t_{22}\delta-t_{21}\delta^2\\ t_{21} & t_{22}-t_{21}\delta\end{bmatrix}\ , \tag{2.11}$$

with $\delta=\delta z/a$. This shows that t_{12} can often be neglected by changing the effective interface position within the distance of the order of the lattice constant. That is, t_{12} essentially describes a shift of the effective interface position.

If we know the interface matrix T_{BA}, we can immediately obtain the interface matrix for the configuration obtained by a mirror reflection at $z=0$, i.e., T_{AB}. This relation depends on the symmetry of the Bloch wave function at the band extremum. For the connection between the conduction bands with s-like symmetry, we have

$$T_{AB}=\begin{bmatrix}1 & 0\\ 0 & -1\end{bmatrix}T_{BA}^{-1}\begin{bmatrix}1 & 0\\ 0 & -1\end{bmatrix}\ . \tag{2.12}$$

The same holds for the connection between the valence bands, both of which have the p symmetry. In the case of the connection between the conduction and valence bands or between the valence and conduction bands, on the other hand, we have

$$T_{AB}=-\begin{bmatrix}1 & 0\\ 0 & -1\end{bmatrix}T_{BA}^{-1}\begin{bmatrix}1 & 0\\ 0 & -1\end{bmatrix}\ . \tag{2.13}$$

The extra minus sign is due to the change in the sign of the valence-band Bloch function with p symmetry under reflection at $z=0$.

In the present formalism all the effects arising from the presence of interfaces have been included in the form of boundary conditions and band offsets. It is based on the assumption that the length scale for spatial variation of envelope functions is much larger than that for abrupt variation of atomic potential and wave functions in the vicinity of the interface. That is, perturbations due to the presence of interfaces such as a potential change due to local charge transfer and mixings of evanescent waves should be confined within the range of a few lattice constants. This seems to be valid in typical heterostructures like GaAs/Al_xGa_{1-x}As (Refs. 10–14) and is expected to be true in other systems. Note that a similar formalism can be applied to optical phonons.[49]

For a given energy, there are many solutions of the Schrödinger equation. Among these solutions, only traveling Bloch functions are allowed in bulk because of boundary conditions. All other solutions are evanescent waves whose amplitude decays or increases exponentially in certain directions. Evanescent waves appear often in association with extremum points in the bulk band structure and their number depends on models of the band structure.[50] (Consider a pseudopotential model, for example. If we expand the wave function in terms of plane waves with reciprocal wave vectors parallel to the interface, the resulting Schrödinger equation becomes a set of coupled second-order differential equations. The number of independent solutions is, therefore, twice that of these equations, i.e., that of the basis plane waves.) In the presence of interface, the total wave function should be expanded in terms of Bloch functions expressed by envelope functions in the vicinity of band extrema and evanescent waves which decay exponentially away from the interface. The interface matrix can then be calculated by matching them at the interface.

The matching conditions can generally be written in a form of the system of linear equations:

$$W_B^{(+)}\begin{bmatrix}\zeta_B\\ \nabla\zeta_B\\ \eta_B^{(+)}\\ \cdots\end{bmatrix}=W_A^{(-)}\begin{bmatrix}\zeta_A\\ \nabla\zeta_A\\ \eta_A^{(-)}\\ \cdots\end{bmatrix}\ , \tag{2.14}$$

with $W_A^{(-)}$ and $W_B^{(+)}$ being appropriate matrices. The quantities $\eta_A^{(-)}$, etc. are coefficients for evanesencent waves $\chi_A^{(-)}$, etc. which decay exponentially away from

the interface in the negative z direction, while $\eta_B^{(+)}$, etc. are those of evanescent waves $\chi_B^{(+)}$, etc. which decay exponentially in the positive z direction. When we consider another interface which is obtained by a mirror reflection at $z=0$, the boundary conditions are still given by equations having the same form as Eq. (2.14), where $W_A^{(-)}$ and $\eta_A^{(-)}$, etc. are replaced by $W_A^{(+)}$ and $\eta_A^{(+)}$, etc. and $W_B^{(+)}$ and $\eta_B^{(+)}$, etc. are replaced by $W_B^{(-)}$ and $\eta_B^{(-)}$, etc. Usually, $W^{(+)}$'s are different from corresponding $W^{(-)}$'s.

We can deduce some general features of the interface matrix without making explicit calculations. Consider one-dimensional systems. In one dimension, there are only two solutions for a given energy and, therefore, no evanescent waves appear in the above equation. There are many cases in which $W^{(+)}$'s are the same as corresponding $W^{(-)}$'s, i.e.,

$$W_A^{(+)}=W_A^{(-)}=W_A \quad \text{and} \quad W_B^{(-)}=W_B^{(+)}=W_B \ . \tag{2.15}$$

In this case we have $T_{BA}=W_B^{-1}W_A$ and $T_{AB}=W_A^{-1}W_B$, i.e., $T_{AB}=T_{BA}^{-1}$. The combination of this relation with Eqs. (2.12) and (2.13) gives the conclusion that the interface matrix is purely diagonal, or $t_{12}=t_{21}=0$, in the case of the connection of band extrema with the same symmetry, and that it is purely off-diagonal, or $t_{11}=t_{22}=0$, in the case of the connection between different symmetry bands.

This feature that the interface matrix is close to a purely diagonal or purely off-diagonal matrix is expected to prevail even in three dimensions as long as contributions of evanescent waves do not play any critical roles. This is actually the case in many heterostructures. In $GaAs/Al_xGa_{1-x}As$ heterostructures, for example, the tight-binding model considered in Sec. III gives a purely diagonal interface matrix as long as the interface or matching plane is chosen at the interfacial As atomic plane. The interface matrix is still nearly diagonal in the pseudopotential model considered in Sec. IV, in which evanescent waves are explicitly taken into account.

III. SIMPLEST TIGHT-BINDING MODEL

One of the simplest models, in which we can calculate boundary conditions, is a chain of atoms having a single s orbital.[41,47] Unfortunately, this model is not appropriate for describing main features of the band structure of III-V compound semiconductors. We adopt a linear-chain model consisting of two kinds of atoms in a unit cell.[51] As is shown in Fig. 1, the unit cell with the width $a/2$ contains an s atomic orbital with energy E_0 and a p orbital with E_1. In the case of GaAs, for example, Ga corresponds to E_0 and As to E_1. We assume only the transfer integral t between nearest-neighbor atoms.

The equation of motion is given by

$$\begin{aligned} &E_1C_1(n)-tC_0(n)+tC_0(n+1)=EC_1(n) \ , \\ &E_0C_0(n+1)+tC_1(n)-tC_1(n+1)=EC_0(n+1) \ . \end{aligned} \tag{3.1}$$

This can readily be solved by setting $C_0(n)=C_0\exp[ik(n-\frac{3}{4})a/2]$ and $C_1(n)=C_1\exp[ik(n-\frac{1}{4})a/2]$. When the energy is close to the bottom of the conduction band, E_0, and the top of the valence band, E_1, we have $E=E_0+(\hbar^2k^2/2m)$ and $E=E_1-(\hbar^2k^2/2m)$, respectively, where $m=2\hbar^2E_g/t^2a^2$ with the band gap $E_g=E_0-E_1$. The envelope function is related to the wave function through

$$\begin{aligned} &C_0(l+1)=\zeta(a/8)\approx\zeta(0)+\tfrac{1}{8}\nabla\zeta(0) \ , \\ &C_1(l)=\frac{t}{2E_g}\nabla\zeta(-a/8)\approx\frac{t}{2E_g}\nabla\zeta(0) \end{aligned} \tag{3.2}$$

when $E\approx E_0$, and

$$\begin{aligned} &C_0(l+1)=\frac{t}{2E_g}\nabla\zeta(a/8)\approx\frac{t}{2E_g}\nabla\zeta(0) \ , \\ &C_1(l)=\zeta(-a/8)\approx\zeta(0)-\tfrac{1}{8}\nabla\zeta(0) \end{aligned} \tag{3.3}$$

when $E\approx E_1$.

At the interface shown in Fig. 1, the equation of motion is explicitly written as

$$\begin{aligned} &E_1^{AB}C_1^A(l)-t_AC_0^A(l)+t_{AB}C_0^B(l+1)=EC_1^A(l) \ , \\ &E_0^{AB}C_0^B(l+1)+t_{AB}C_1^A(l)-t_BC_1^B(l+1)=EC_0^B(l+1) \ . \end{aligned} \tag{3.4}$$

By subtracting the corresponding equation in bulk from the above, we get the boundary conditions

$$\begin{aligned} &t_{AB}C_0^B(l+1)=t_AC_0^A(l+1)-(E_1^{AB}-E_1^A)C_1^A(l) \ , \\ &t_BC_1^B(l)-(E_0^{AB}-E_0^B)C_0^B(l+1)=t_{AB}C_1^A(l) \ , \end{aligned} \tag{3.5}$$

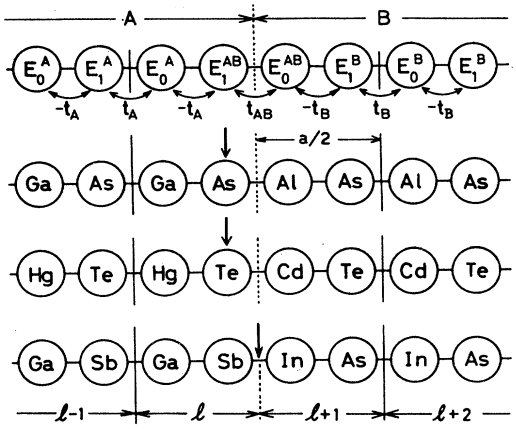

FIG. 1. The linear chain model consisting of a cation s and an anion p_z atomic orbital. E_0 and E_1 represent the energy of the s and p_z orbital, respectively, and t the transfer integral between a nearest-neighbor pair. The length of the unit cell is half of the lattice constant of III-V semiconductors. At the interface of A and B, the transfer integral t_{AB} and energies of interfacial atoms, E_0^{AB} and E_1^{AB}, can be different from those in bulk. In case of $GaAs/Al_xGa_{1-x}As$ heterostructures, the interface position z_0 is chosen at that of the interfacial As atom, and in the case of HgTe/CdTe the interface is at that of the interfacial Te atom. In the case of GaSb/InAs heterostructures, on the other hand, the interface is chosen at the center of the Sb—In bond.

where $C_0^A(l+1)$ and $C_1^B(l)$ are the extrapolated values past the interface from left and right, respectively. The boundary conditions for the envelope, i.e., the interface matrix T_{BA}, can easily be obtained if we substitute Eqs. (3.2) or (3.3) into Eq. (3.5) depending on which band extrema are close to each other in energy.

A. Connection between conduction bands

When the bottom of the conduction band of the semiconductor A is close to that of B, we can safely assume that $E_0^{AB} \approx E_0^A \approx E_0^B$. The interface matrix becomes

$$t_{11}=\frac{t_A}{t_{AB}}, \quad t_{22}=\frac{t_{AB}t_A E_g^B}{t_B^2 E_g^A}, \quad t_{21}=0 ,$$
$$t_{12}=\frac{t_A}{t_{AB}}-\frac{t_A t_{AB} E_g^B}{t_B^2 E_g^A}-\frac{4t_A(E_1^{AB}-E_0^A)}{t_{AB}E_g^A} . \tag{3.6}$$

This reduces exactly to that assumed in the EFA when the transfer integrals, t_A, t_B, and t_{AB}, are all equal, because t_{12} can be eliminated by an appropriate choice of the interfacial position as has been discussed in the previous section. Therefore, the validity of the EFA does not require the equivalence of the Bloch functions at the conduction-band bottom but that of effective transfer integrals closely related to momentum matrix elements between the conduction-band bottom and the valence-band top. For usual III-V compound semiconductors, the transfer integrals or the momentum matrix elements are of the same order of magnitude,[52] and therefore the boundary conditions are not so much different from those assumed in the EFA.

One of the typical examples is GaAs/Al_xGa_{1-x}As heterostructures. In this system, we have $t_{AB}=t_B$, and also $E_1^{AB}-E_1^A \approx (E_g^A-E_g^B)/2$, by assuming the simple average $E_1^{AB}=(E_1^A+E_1^B)/2$. Further, it is reasonable to choose the interface position at the interfacial As atom, which can easily be achieved by substituting $\delta z=-a/8$ in the formula (2.11). We can express the interface matrix in terms of the band gaps and the effective masses as

$$\tilde{T}_{BA}=\begin{bmatrix}(m_B E_g^A/m_A E_g^B)^{1/2} & 0 \\ 0 & (m_A E_g^B/m_B E_g^A)^{1/2}\end{bmatrix} . \tag{3.7}$$

For small Al contents x, we can usually write as $m(x)=m(1+\alpha x)$ and $E_g(x)=E_g(1+\beta x)$ with $m \approx 0.066 m_0$, $E_G \approx 1.519$ eV, $\alpha \approx 0.895$, and $\beta \approx 1.333$.[53] Therefore, we have

$$\tilde{T}_{BA} \approx \begin{bmatrix}1+\gamma x & 0 \\ 0 & 1-\gamma x\end{bmatrix}, \quad \gamma=(\alpha-\beta)/2 \approx 0.22 \tag{3.8}$$

with $x=x_B-x_A$, where x_A and x_B are the Al content of the left (A) and right (B) material. The interface matrix (3.7) has already been used for self-consistent calculation of energy levels and for evaluation of scattering mechanisms at low temperatures in single heterojunctions.[54]

B. Connection between light-hole valence bands

When the top of the valence band of A and B is close in energy, i.e., $E_1^A \approx E_1^B$, we have $E_1^{AB} \approx E_1^A$ and

$$t_{11}=\frac{t_{AB}}{t_B}, \quad t_{22}=\frac{t_A^2 E_g^B}{t_{AB}t_B E_g^A}, \quad t_{21}=0 ,$$
$$t_{12}=-\frac{1}{8}\left[\frac{t_{AB}}{t_B}-\frac{t_A^2 E_g^B}{t_{AB}t_B E_g^A}-\frac{4t_A^2(E_0^{AB}-E_0^B)}{t_{AB}t_B E_g^A}\right] . \tag{3.9}$$

Again, in the case of GaAs/Al_xGa_{1-x}As systems, we have $t_{AB}=t_B$, $E_0^{AB} \approx E_0^B$, and

$$T_{BA}=\begin{bmatrix}1 & 0 \\ 0 & m_B/m_A\end{bmatrix} \text{ or } \tilde{T}_{BA}=\begin{bmatrix}1 & 0 \\ 0 & 1\end{bmatrix} , \tag{3.10}$$

where the interface is chosen at the position of the interfacial As atom. This shows that the EFA is exact for connection between light-hole valence bands in GaAs/Al_xGa_{1-x}As systems.

The reason that the EFA is exact for connection between valence bands and not for that between conduction bands is easily understood. In GaAs/Al_xGa_{1-x}As systems, the interfacial As atom is common to both materials and therefore the amplitude of the p symmetry orbital of As connects continuously across the interface. This means that the envelope $\zeta(z)$ itself is continuous for connection between the valence bands and that the quantity $t\nabla\zeta/E_g$ is continuous for connection between the conduction bands.

Another example is HgTe/CdTe systems in which HgTe is known to have a so-called inverted-band structure.[55,56] In the case of HgTe, E_0 of the s-like orbital of Hg is lower in energy than E_1 of the p-like orbital of Te. Therefore, the p-like orbital of Te constitutes the conduction band and the s-like orbital of Hg the valence band in contrast to CdTe and usual III-V semiconductors. In this case, we have to connect envelope functions associated with the conduction band (p symmetry) of HgTe (A) and the light-hole valence band (p symmetry) of CdTe (B). We have $t_{AB}=t_B$ and also $E_0^{AB} \approx E_0^B$. Choosing the interface position at the interfacial Te atom, we have

$$T_{BA}=\begin{bmatrix}1 & 0 \\ 0 & -m_B/m_A\end{bmatrix} \text{ or } \tilde{T}_{BA}=\begin{bmatrix}1 & 0 \\ 0 & -1\end{bmatrix} . \tag{3.11}$$

The negative sign in t_{22} reflects the difference of the dispersion of the conduction and valence bands.

C. Connection between conduction and valence bands

Since the results are complicated, the expressions only in the case $E_0^{AB} \approx E_0^B$ and $E_1^{AB} \approx E_1^A$ will be given. For the connection between the valence band of A and the conduction band of B, we have

$$T_{BA}=\begin{bmatrix}-t_{AB}E_g^B/4t_B^2 & t_A^2/2t_{AB}E_g^A+t_{AB}E_g^B/32t_B^2 \\ 2t_{AB}E_g^B/t_B^2 & -t_{AB}E_g^B/4t_B^2\end{bmatrix} . \tag{3.12}$$

For the connection between the conduction band of A and the valence band of B, on the other hand, we have

$$T_{BA}=\begin{bmatrix} t_A E_g^B/4t_{AB}t_B & t_A t_{AB}/2t_B E_g^A + t_A E_g^B/32 t_{AB} t_B \\ 2t_A E_g^B/t_{AB}t_B & t_A E_g^B/4t_{AB}t_B \end{bmatrix} . \tag{3.13}$$

A typical example is GaSb/InAs, where the bottom of the conduction band of InAs lies below the top of the valence band of GaSb and the envelopes associated with the s-like conduction band of InAs and the p-like valence band of GaSb should be connected at the interface. This class of materials was first examined theoretically by Sai-Halasz *et al.*,[51] experimentally by Sakaki *et al.*,[57,58] and has been extensively studied since.[59] There can exist two kinds of interfaces, i.e., that consisting of Sb—In bonds and that of Ga—As bonds. The latter interface matrix, denoted by $T(\mathrm{In}\mathit{As}\leftarrow\mathit{Ga}\mathrm{Sb})$, can be directly obtained from Eq. (3.12), while the former, denoted by $T(\mathit{In}\mathrm{As}\leftarrow\mathrm{Ga}\mathit{Sb})$, can be obtained from Eq (3.13) using the symmetry relation Eq. (2.13).

Explicit results can be obtained if the transfer integrals t_A, t_B, and t_{AB} are estimated by the known effective masses, band gaps, and lattice constants of bulk InAs, GaSb, InSb, and GaAs. Using the parameters given in Table I, we have

$$T(\mathrm{In}\mathit{As}\leftarrow\mathit{Ga}\mathrm{Sb})=\begin{bmatrix} 0.033 & 2.113 \\ 0.268 & 0.033 \end{bmatrix} ,$$
$$T(\mathit{In}\mathrm{As}\leftarrow\mathrm{Ga}\mathit{Sb})=\begin{bmatrix} -0.038 & 1.850 \\ 0.306 & -0.038 \end{bmatrix} . \tag{3.14}$$

The two interfaces Ga-As and Sb-In give results different from each other but the difference is not so appreciable. Since the diagonal elements of both interface matrices are small in comparison with off-diagonal elements, the boundary conditions are such that the amplitude of B is determined by the derivative of A and the derivative of B is determined by the amplitude of A.

The envelope-function approximation can also be extended to GaSb/InAs systems. Bastard has used a $\mathbf{k}\cdot\mathbf{p}$ Hamiltonian containing terms linear in wave vector based on an s-like conduction band and three p-like valence bands and proposed that coefficients (envelopes) for all these band extrema should be continuous across the interface.[35] In the present context, this assumption leads to the following boundary conditions:

TABLE I. Parameters used for the present calculation: a is the lattice constant, E_g the band gap, m the effective mass, and t the transfer integral.

Material	a (Å)	E_g (eV)	m/m_0	t (eV)
GaAs	5.653	1.52	0.066	3.288
GaSb	6.095	0.78	0.042	2.759
InAs	6.058	0.44	0.024	2.758
InSb	6.479	0.27	0.014	2.645

$$\zeta_B(0)=\frac{t_A}{2E_g^A}\nabla\zeta_A(0) \quad \text{and} \quad \frac{t_B}{2E_g^B}\nabla\zeta_B(0)=\zeta_A(0) . \tag{3.15}$$

The interface matrix becomes

$$T_{BA}=\begin{bmatrix} 0 & t_A/2E_g^A \\ 2E_g^B/t_B & 0 \end{bmatrix} , \tag{3.16}$$

independent of whether the interface consists of Ga-As or Sb-In atoms. Note that the flux conservation is satisfied only when the transfer integrals of A and B are the same, i.e., $t_A=t_B$. Using the parameters given in Table I, we have

$$T_{BA}=\begin{bmatrix} 0 & 1.769 \\ 0.319 & 0 \end{bmatrix} . \tag{3.17}$$

which are close to Eq. (3.14).

Strictly speaking, these interface matrices are not directly applicable to the case of nonzero k_x or k_y. The top of the valence band is described by p symmetry orbitals and is highly degenerate.[1] For $k_x=k_y=0$, the conduction band of InAs couples only with the light-hole valence band of GaSb with the p_z symmetry. For nonzero k_x or k_y it can couple with the heavy-hole valence bands with p_x or p_y symmetry. Such couplings with heavy holes are proportional to $k_x a$ or $k_y a$ and are expected to be unimportant as long as $k_x a \ll 1$ and $k_y a \ll 1$.

IV. SIMPLEST PSEUDOPOTENTIAL MODEL

As is well known, the pseudopotential of GaAs, for example, is written as[60]

$$V(\mathbf{r})=\sum_{\mathbf{G}} (V_{\mathbf{G}}^S \cos\mathbf{G}\cdot\tau + iV_{\mathbf{G}}^A \sin\mathbf{G}\cdot\tau)\exp[i\mathbf{G}\cdot(\mathbf{r}+\tau)] , \tag{4.1}$$

with $\mathbf{G}$ the reciprocal lattice vector and $\tau=(1,1,1)(a/8)$, where the origin $\mathbf{r}=\mathbf{0}$ is chosen at an As atom and 2τ is a vector directing from the As atom to a Ga atom. For simplicity, we consider only the six parameters V_3^S, V_8^S, V_{11}^S, V_3^A, V_4^A, and V_{11}^A, where $V_3^S=V_{\mathbf{G}}^S$ with $\mathbf{G}=(1,1,1)(2\pi/a)$, $V_8^S=V_{\mathbf{G}}^S$ with $\mathbf{G}=(2,2,0)(2\pi/a)$, etc. As the plane-wave basis, we similarly confine ourselves to 15 waves satisfying $|\mathbf{G}|\le 4\pi/a$. When we consider the conduction band for $k_x=k_y=0$ with the Δ_1 symmetry, we have only eight independent waves ξ_0, $\xi_0\exp(\pm 4\pi i z/a)$, $\xi_1\exp(\pm 2\pi i z/a)$, $\xi_2\exp(\pm 2\pi i z/a)$, and ξ_3, where $\xi_j(x,y)$ with $j=0,\ldots,3$, defined by

$$\xi_0(x,y)=1\ ,$$
$$\xi_1(x,y)=2\cos\left[\frac{2\pi x}{a}\right]\cos\left[\frac{2\pi y}{a}\right]\ ,$$
$$\xi_2(x,y)=2\sin\left[\frac{2\pi x}{a}\right]\sin\left[\frac{2\pi y}{a}\right]\ , \tag{4.2}$$
$$\xi_3(x,y)=\cos\left[\frac{4\pi x}{a}\right]+\cos\left[\frac{4\pi y}{a}\right]\ ,$$

constitute the basis in the xy plane.

As the pseudopotential parameters of GaAs and AlAs, we use those proposed by Baldereschi *et al.*[61] and the arithmetic average of those of GaAs and AlAs for $Al_xGa_{1-x}As$ (virtual crystal approximation), i.e.,

$$V(Al_xGa_{1-x}As)=(1-x)V(GaAs)+xV(AlAs)\ . \tag{4.3}$$

In this model, the conduction-band minimum is located at the Γ point for $x<0.31$. In the following we confine ourselves to this range of x. Figure 2 gives the band structure of bulk GaAs and AlAs calculated in the present model. We immediately notice insufficiency of the number of basis plane waves. For GaAs, for example, the band gap is $E_g\approx 1.13$ eV instead of known 1.52 eV and the effective mass at the Γ conduction-band minimum is $m\approx 0.060m_0$ instead of known $0.066m_0$.[62]

The interface matrix T_{BA} is determined by the continuity of the wave function and its derivative at the matching plane $z=z_0$,

$$\psi_B(x,y,z_0)=\psi_A(z,y,z_0)\ ,$$
$$\frac{\partial}{\partial z}\psi_B(x,y,z_0)=\frac{\partial}{\partial z}\psi_A(z,y,z_0)\ . \tag{4.4}$$

The wave function of each side consists of the Bloch function associated with the minimum of the conduction band and evanescent waves decaying exponentially away from the interface. The procedure is analogous to that employed by Sham and Nakayama[63] in calculating valley splittings of Si inversion layers and that used by Marsh and Inkson[46] in calculating reflection coefficients from $GaAs/Al_xGa_{1-x}As$ single interfaces. According to the $\mathbf{k}\cdot\mathbf{p}$ theory,[1] the wave function at $k_x=k_y=0$ is expressed by the envelope through

$$\psi(\mathbf{r})=\psi_0(\mathbf{r})\zeta(z)+\psi_0'(\mathbf{r})\nabla\zeta(z)\ , \tag{4.5}$$

where $\psi_0(\mathbf{r})$ is the Bloch function of the conduction-band minimum at the Γ point and $\psi_0'(\mathbf{r})$ is its change to the lowest order in k_z. We have

$$\psi_0'(\mathbf{r})=-ia^{-1}\sum_{j\neq 0}\psi_j(\mathbf{r})\frac{\hbar(j|p_z|0)}{m_0(\varepsilon_j-\varepsilon_0)}\ , \tag{4.6}$$

where $\psi_j(\mathbf{r})$ and ε_j are the Bloch function and the energy at the Γ point ($j=0$ being the conduction-band bottom), and $(j|p_z|0)$ is the matrix element of the momentum in the z direction.

Since there are four independent basis functions in the xy plane, the above (4.4) constitutes eight independent equations. In each side of the interface, we have to include three evanescent waves with a complex wave vector κ decaying exponentially away from the matching plane $z=z_0$ in addition to the wave function given by Eq. (4.5) described in terms of the envelope function $\zeta(z)$. Then, Eq. (4.4) determines ζ_B and $\nabla\zeta_B$ as well as amplitudes of six evanescent waves for a given set of ζ_A and $\nabla\zeta_A$.

The evanescent waves should be determined in such a way that the real part of their wave vector should be inside of the first Brillouin zone. Actual calculations for $Al_xGa_{1-x}As$ at the energy of the Γ conduction-band minimum give an evanescent wave χ_0 having a wave vector with a vanishing real part and two waves χ_+ and χ_-, each of which has a wave vector whose real part is very close to the position of an additional extremum in the vicinity of an X point. As is clear in Fig. 2, however, the conduction-band minima in the vicinity of X points are slightly outside of the first Brillouin zone (about 10% of the distance between Γ and X points), partly due to the insufficiency of the number of basis waves in the present simplest model. Consequently, the real part of the complex wave vector of χ_+ and χ_- is slightly larger than $2\pi/a$ or smaller than $-2\pi/a$. (For GaAs, for example, we have $\kappa_0 a/2\pi\approx 1.37i$ and $\kappa_\pm a/2\pi\approx\pm 1.08+0.28i$.) It is expected, however, that the present calculation still provides characteristic features of the boundary conditions in spite of such slight inadequacies.

In addition to the interface matrix connecting the envelopes of both sides, the amplitude of the evanescent waves are also determined at the same time. Let η_j ($j=0,+,-$) be the coefficients for the evanescent waves χ_j. Then we can write

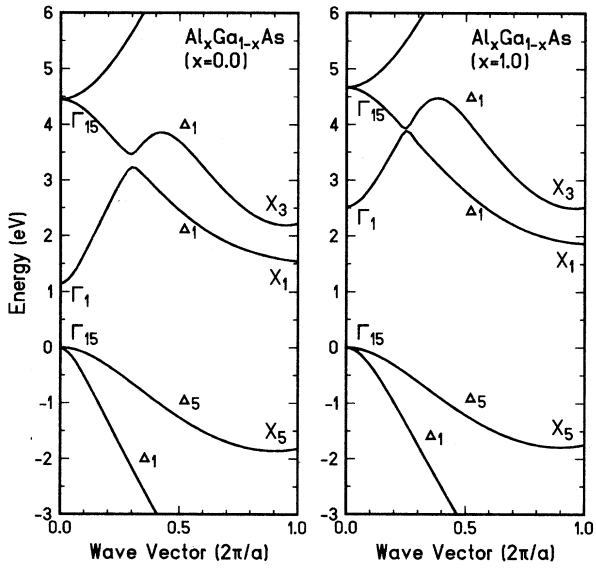

FIG. 2. The band structure of GaAs and AlAs along the Δ axis [$\mathbf{k}=(0,0,k_z)$, $0\le k_z\le 2\pi/a$] calculated in the empirical pseudopotential model. The energy origin is at the top of the valence band Γ_{15}. Because of the insufficiency in the number of basis plane waves, the band gap of GaAs at the Γ point is slightly smaller than the known value, and the extrema in the vicinity of X points are slightly outside of the first Brillouin zone.

$$\begin{bmatrix} \eta_0^B \\ \eta_+^B \\ \eta_-^B \end{bmatrix} = \tilde{P} \begin{bmatrix} \zeta_A \\ \nabla_A \zeta_A \end{bmatrix} \quad \text{and} \quad \begin{bmatrix} \eta_0^A \\ \eta_+^A \\ \eta_-^A \end{bmatrix} = \tilde{Q} \begin{bmatrix} \zeta_A \\ \nabla_A \zeta_A \end{bmatrix} , \tag{4.7}$$

where $\tilde{P}=(p_{ij})$ and $\tilde{Q}=(q_{ij})$ are a 3×2 matrix. Clearly, these matrices depend on the choice of the amplitude of evanescent waves because they are not normalizable in bulk. Here, we choose the amplitude in such a way that

$$\sum_{i=0}^{3} \left| \int\int \xi_i(x,y,z_0)^* \chi_j(x,y,z_0) dx\, dy \right|^2 = 1 . \tag{4.8}$$

Because of the symmetry we can choose the matrix $\tilde{P}$ such that

$$p_{01}^* = p_{01}, \quad p_{02}^* = p_{02}, \quad p_{-1} = p_{+1}^*, \quad \text{and } p_{-2} = p_{+2}^* . \tag{4.9}$$

The same holds for the matrix $\tilde{Q}$.

Examples of calculated diagonal matrix elements of the interface matrix, $\tilde{t}_{11}$ and $\tilde{t}_{22}$, are given in Fig. 3 and off-diagonal elements, $\tilde{t}_{12}$ and $\tilde{t}_{21}$, in Fig. 4 for $GaAs/Al_xGa_{1-x}As$ as a function of the position z_0 of the matching plane. Coefficients for evanescent waves are given in Fig. 5. The interfacial As plane is at $z_0=0$, and the adjacent Ga and (Ga,Al) planes are at $z_0=-a/4$ and $z_0=a/4$, respectively. The resulting matrices are all periodic in z_0 with the period $a/2$. We see immediately that the off-diagonal elements are negligibly small. The diagonal elements $\tilde{t}_{11}$ and $\tilde{t}_{22}$ deviate slightly from unity

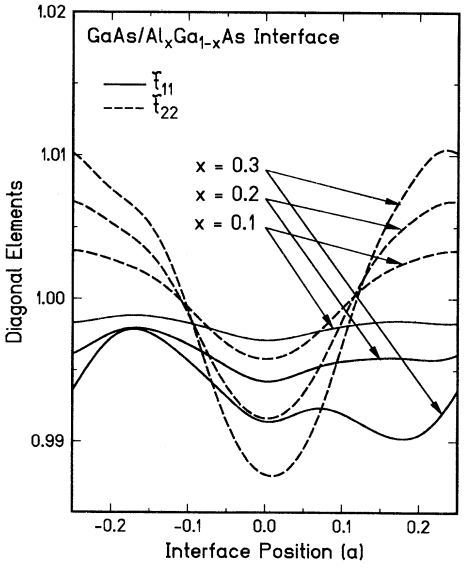

FIG. 3. Calculated diagonal elements $\tilde{t}_{11}$ and $\tilde{t}_{22}$ of the interface matrix $\tilde{T}_{BA}$ for $GaAs/Al_xGa_{1-x}As$ heterostructures as a function of the interface position z_0. The origin $z_0=0$ is at the interfacial As atomic plane. The solid and dashed lines represent $\tilde{t}_{11}$ and $\tilde{t}_{22}$, respectively. The position of a Ga atomic plane is at $z_0=-a/4$ and that of an (Al,Ga) plane at $z_0=a/4$.

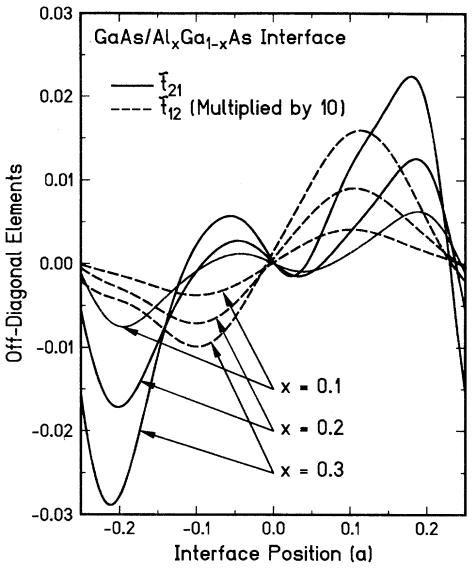

FIG. 4. Calculated off-diagonal elements $\tilde{t}_{12}$ and $\tilde{t}_{21}$ of the interface matrix $\tilde{T}_{BA}$ for $GaAs/Al_xGa_{1-x}As$ heterostructures as a function of the interface position z_0. The solid lines represent $\tilde{t}_{21}$ and the dashed lines $10\tilde{t}_{12}$.

in proportion to x, but the proportionality coefficient depends on the interface position z_0. Therefore, it is impossible to determine T_{BA} uniquely, although we can safely conclude that the EFA works surprisingly well for the Γ conduction-band minimum of $GaAs/Al_xGa_{1-x}As$ heterostructures. Mixings of evanescent waves associated with X conduction-band minima are small but also exhibit dependence on z_0. Note that the off-diagonal elements

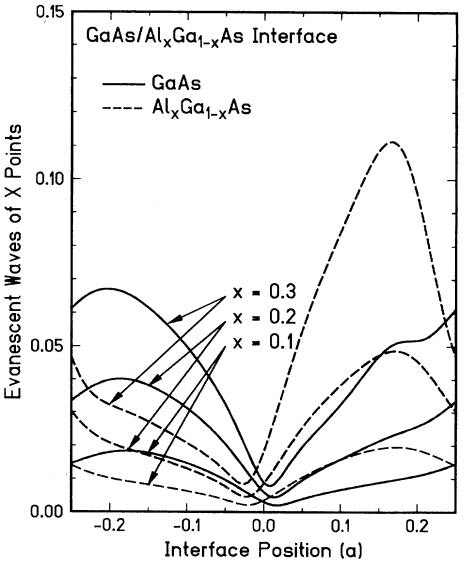

FIG. 5. Calculated mixings of evanescent waves associated with X point minima. The solid and dashed lines represent the coefficients $|p_{+1}|$ and $|q_{+1}|$, respectively, for the amplitude of the envelope $\zeta(z_0)$.

$\tilde{t}_{12}$ and $\tilde{t}_{21}$ (and mixings of evanescent waves also) become small when the matching plane is at the interfacial As atomic plane, i.e., at $z_0=0$. This is in accord with the symmetry argument given in the last paragraphs of Sec. II.

The calculated $|\tilde{t}_{21}|$ is at most 0.03 even for $x=0.3$, which means $|t_{21}|<0.002$ because $t_{21}=(m_B/m_0)\tilde{t}_{21}$. Therefore, the dependence of $\tilde{t}_{11}$ and $\tilde{t}_{22}$ on the interface position z_0 is not affected by the choice of the interface position in the sense expressed by Eq. (2.11). Instead it originates from the present assumption that the potential changes abruptly from that of GaAs to that of $Al_xGa_{1-x}As$ at $z=z_0$ as clearly shown in Eq. (4.4). This unphysical discontinuity of the potential certainly depends strongly on z_0. In actual interfaces the potential changes from that of GaAs to $Al_xGa_{1-x}As$ smoothly within the distance of the order of the lattice constant. Effects of such smooth changes in the potential cannot be described by the solutions in bulk alone. We have to introduce two matching planes on both sides sufficiently away from the interface, where the potential is almost exactly equal to that in bulk, and then solve the Schrödinger equation explicitly between the two matching planes.

The dependence on the position of the matching plane makes it difficult to give definite conclusions on deviations from the EFA. It can nevertheless be seen that $\tilde{t}_{11}$ depends on the interface position only weakly and decreases with increasing x. This deviation from the EFA is in the opposite direction from that obtained in the linear-chain tight-binding model considered in the previous section [see Eq. (3.8)]. The situation does not change even if a more elaborate tight-binding model is used,[48] which will be discussed in more detail in the following paper. This shows that reliable and very elaborate calculations are required in discussing possible deviations of boundary conditions from the EFA.

The calculated interface matrix violates the flux conservation condition $\det\tilde{T}_{BA}=1$, because the product $\tilde{t}_{11}\tilde{t}_{22}$ can be smaller and larger than unity ($\tilde{t}_{12}\tilde{t}_{21}$ is negligible). This is presumably due to the violation of the periodicity in the reciprocal space inherent to the pseudopotential model containing finite numbers of basis plane waves. That is, the truncation of the number of basis plane waves gives rise to the presence of traveling wave solutions with large wave vectors ($|k_z|\gg 2\pi/a$), and some part of the incident flux is likely to be carried away by such unphysical traveling waves at the interface. The actual amount of the violation is very small and unimportant.

V. SUMMARY AND CONCLUSION

We have studied the boundary conditions for envelope functions appearing in the effective-mass approximation at heterointerfaces. The boundary conditions have been expressed by the 2×2 interface matrix T_{BA} which gives linear relations among envelopes and their first derivatives at the interface. We have used two simple models, the linear-chain tight-binding model, which can describe essential features of the conduction and light-hole valence bands in the vicinity of the Γ point, and an empirical pseudopotential model.

In the former model, we have calculated the interface matrix for all types of connections. It has turned out that the calculated boundary conditions are very similar to those assumed in the envelope-function approximation (EFA) in all the cases considered. Especially in calculating energy levels, deviations from the EFA are negligible in comparison with more important effects such as uncertainty in band offset or barrier height and nonparabolicity.

In the latter pseudopotential model, the interface matrix for the connection of Γ-valley conduction-band envelope functions of GaAs and $Al_xGa_{1-x}As$ has been calculated. It has been shown that deviation from the EFA, although very small, depends on the position of the matching plane or the interface. Within such uncertainty of calculations, the results again justify the validity of the EFA.

In the following paper, the interface-matrix formalism is extended so as to explicitly treat problems arising from mixings of Γ- and X-valley minima in GaAs/$Al_xGa_{1-x}As$ heterostructures.

ACKNOWLEDGMENTS

One of the authors (T.A.) thanks Dr. Shojiro Mori for collaboration in a part of the present work (some parts of Secs. II and III) at the early stage. This work is supported in part by Grant-in-Aid for Specially Promoted Research from the Ministry of Education, Science and Culture, Japan.

[1] J. M. Luttinger and W. Kohn, Phys. Rev. **97**, 869 (1955).
[2] L. Esaki and R. Tsu, IBM J. Res. Dev. **14**, 61 (1970).
[3] See, for example, H. Kroemer, Surf. Sci. **174**, 299 (1986), and references therein.
[4] D. C. Tsui, H. L. Stormer, and A. C. Gossard, Phys. Rev. Lett. **48**, 1559 (1982).
[5] T. Mimura, S. Hiyamizu, T. Fujii, and K. Nanbu, Jpn. J. Appl. Phys. **19**, L225 (1980).
[6] J. P. van der Ziel, R. Dingle, R. C. Miller, W. Wiegmann, and W. A. Nordland, Jr., Appl. Phys. Lett. **26**, 463 (1975).
[7] L. L. Chang, L. Esaki, and R. Tsu, Appl. Phys. Lett. **24**, 593 (1974).
[8] T. C. L. G. Sollner, W. D. Goodhue, P. E. Tannenwald, C. D. Parker, and D. Peck, Appl. Phys. **43**, 588 (1983).
[9] N. Yokoyama, K. Imamura, S. Muto, S. Hiyamizu, and H. Nishi, Jpn. J. Appl. Phys. **24**, L853 (1985).
[10] W. E. Pickett, S. G. Louie, and M. L. Cohen, Phys. Rev. B **17**, 815 (1978); J. Vac. Sci. Technol. **15**, 1437 (1978).
[11] J. Sanchez-Dehesa and C. Tejedor, Phys. Rev. B **26**, 5824 (1982).

[12]T. Nakayama and H. Kamimura, J. Phys. Soc. Jpn. **54**, 4726 (1985); H. Kamimura and T. Nakayama, in *Proceedings of the 18th International Conference on the Physics of Semiconductors, Stockholm, 1986,* edited by O. Engström (World Scientific, Singapore, 1987), p. 643; Comments Condensed Matter Phys. **13**, 143 (1987); T. Nakayama, Ph.D. thesis, University of Tokyo, 1987.

[13]D. M. Wood, S.-H. Wei, and A. Zunger, Phys. Rev. Lett. **58**, 1123 (1987).

[14]N. Hamada and S. Ohnishi, Superlatt. Microstruct. **3**, 301 (1987).

[15]E. Caruthers and P. J. Lin-Chung, J. Vac. Sci. Technol. **15**, 1459 (1978).

[16]W. Andreoni and R. Car, Phys. Rev. B **21**, 3334 (1980).

[17]M. Jaros, K. B. Wong, and M. A. Gell, Phys. Rev. B **31**, 1205 (1985); J. Vac. Sci. Technol. B **3**, 1051 (1985).

[18]K. B. Wong, M. Jaros, M. A. Gell, and D. Ninno, J. Phys. C **19**, 53 (1986).

[19]M. A. Gell, D. Ninno, M. Jaros, and D. C. Herbert, Phys. Rev. B **34**, 2416 (1986).

[20]M. G. Gell, D. Ninno, M. Jaros, D. J. Wolford, T. F. Keuch, and J. A. Bradley, Phys. Rev. B **35**, 1196 (1987).

[21]J. N. Schulman and T. C. McGill, Phys. Rev. Lett. **39**, 1680 (1977); Phys. Rev. B **19**, 6341 (1979); **23**, 4149 (1981).

[22]J. N. Schulman and Y.-C. Chang, Phys. Rev. B **24**, 4445 (1981); **27**, 2346 (1983); **31**, 2056 (1985).

[23]Y.-C. Chang and J. N. Schulman, Phys. Rev. B **25**, 3975 (1982); J. Vac. Sci. Technol. **21**, 540 (1982); Phys. Rev. B **31**, 2069 (1985).

[24]D.Z.-Y. Ting and Y.-C. Chang, Phys. Rev. B **36**, 4359 (1987).

[25]M. K. Mon, Solid State Commun. **41**, 699 (1982).

[26]E. Yamaguchi, J. Phys. Soc. Jpn. **56**, 2835 (1987).

[27]S. Nara, Jpn. J. Appl. Phys. **26**, 690 (1987); **26**, 1713 (1987).

[28]L. Brey and C. Tejedor, Phys. Rev. B **35**, 9112 (1987).

[29]For details of self-consistent calculations in space-charge layers, see, for example, T. Ando, A. B. Fowler, and F. Stern, Rev. Mod. Phys. **54**, 437 (1982).

[30]See also, G. Bastard, Surf. Sci. **170**, 426 (1986), and references therein.

[31]For exciton problems, for example, see G. E. W. Bauer and T. Ando, Phys. Rev. B **38**, 6015 (1988), and references therein.

[32]See, for example, Proceedings of the 7th International Conference on Electronic Properties of Two-Dimensional Systems, edited by J. M. Worlock [Surf. Sci. **196**, 1 (1988)].

[33]W. A. Harrison, Phys. Rev. **123**, 85 (1961).

[34]D. J. Ben Daniel and C. B. Duke, Phys. Rev. **152**, 682 (1966).

[35]G. Bastard, Phys. Rev. B **24**, 5693 (1981); **25**, 7584 (1982).

[36]S. R. White and L. J. Sham, Phys. Rev. Lett. **47**, 879 (1981).

[37]M. Altarelli, Phys. Rev. B **28**, 842 (1983).

[38]R. Eppenga, M. F. H. Schuurmans, and S. Colak, Phys. Rev. B **36**, 1554 (1987).

[39]P. J. Price, in *Proceedings of the International Conference on the Physics of Semiconductors, Exeter, 1962* (Institute of Physics and the Physical Society, London, 1962), p. 99.

[40]S. R. White, G. E. Marques, and L. J. Sham, J. Vac. Sci. Technol. **21**, 544 (1982).

[41]H. Kroemer and Q.-G. Zhu, J. Vac. Sci. Technol. **21**, 551 (1982); Q.-G. Zhu and H. Kroemer, Phys. Rev. B **27**, 3519 (1983).

[42]A. Ishibashi, Y. Mori, K. Kaneko, and N. Watanabe, J. Appl. Phys. **59**, 4087 (1986).

[43]R. A. Morrow and K. R. Brownstein, Phys. Rev. B **30**, 678 (1984); R. A. Morrow, *ibid.* **35**, 8074 (1987); **36**, 4836 (1987). See also, I. Galbraith and G. Duggan, Phys. Rev. B **38**, 10 057 (1988).

[44]W. Trzeciakowski, Phys. Rev. B **38**, 4322 (1988); **38**, 12 493 (1988).

[45]G. C. Osbourn and D. L. Smith, J. Vac. Sci. Technol. **16**, 1529 (1979); Phys. Rev. B **19**, 2124 (1979).

[46]A. C. Marsh and J. C. Inkson, Solid State Commun. **52**, 1037 (1984); J. Phys. C **17**, 6561 (1984); **19**, 43 (1986). See also, S. Collins, D. Lowe, and J. R. Barker, J. Phys. C **18**, L637 (1985); A. C. Marsh, Semicond. Sci. Technol. **1**, 237 (1986).

[47]T. Ando and S. Mori, Surf. Sci. **113**, 124 (1982).

[48]H. Akera, S. Wakahara, and T. Ando, Surf. Sci. **196**, 694 (1988).

[49]T. Tsuchiya, H. Akera, and T. Ando, Phys. Rev. B **39**, 6025 (1989); H. Akera and T. Ando, *ibid.* **40**, 2914 (1989).

[50]For more details on evanescent waves, see Ref. 23 and references therein.

[51]G. A. Sai-Halasz, L. Esaki, and W. A. Harrison, Phys. Rev. B **18**, 2812 (1978).

[52]It is conventionally assumed that $t = C/a^2$ with a the lattice constant, where C is a constant independent of materials. [See, for example, W. A. Harrison, in *Electronic Structure and the Properties of Solids* (Freeman, San Francisco, 1980)].

[53]C. Bosio, J. L. Staehli, M. Guzzi, G. Burri, and R. A. Logan, Phys. Rev. B **38**, 3263 (1988).

[54]T. Ando, J. Phys. Soc. Jpn. **51**, 3893 (1982); **51**, 3900 (1982).

[55]Y. C. Chang, J. N. Schulman, G. Bastard, Y. Guldner, and M. Voos, Phys. Rev. B **31**, 2557 (1985).

[56]Y. R. Lin-Liu and L. J. Sham, Phys. Rev. B **36**, 4836 (1985).

[57]H. Sakaki, L. L. Chang, R. Ludeke, C.-A. Chang, G. A. Sai-Halasz, and L. Esaki, Appl. Phys. Lett. **31**, 211 (1977).

[58]H. Sakaki, L. L. Chang, G. A. Sai-Halasz, C.-A. Chang, and L. Esaki, Solid State Commun. **26**, 589 (1978).

[59]See, for example, L Esaki, IEEE J. Quantum Electron. **QE-22**, 1611 (1986), and references therein.

[60]See, for example, M. L. Cohen and V. Heine, in *Solid State Physics,* edited by H. Ehrenreich, F. Seitz, and D. Turnbull (Academic, New York, 1970), p. 38.

[61]A. Baldereschi, E. Hess, K. Maschke, H. Neumann, K.-R. Schulze, and K. Unger, J. Phys. C **10**, 4709 (1977).

[62]See, for example, J. S. Blakesmore, J. Appl. Phys. **53**, R123 (1982).

[63]L. J. Sham and M. Nakayama, Phys. Rev. B **20**, 734 (1979).